Pergamon

Tetrahedron, Vol. 53, No. 13, pp. 4715-4726, 1997
© 1997 Published by Elsevier Science Ltd
All rights reserved. Printed in Great Britain
0040-4020/97 $17.00 + 0.00

PII: S0040-4020(97)00140-3

1,1-Diphenylethylene Adsorbed onto Acid Zeolites: Nature of the Blue (605-nm) Species

Vicente Fornés,[1] Hermenegildo García,[1]* Slobodan Jovanovic[2] and Vicente Martí[1]

[1] Instituto de Tecnología Química, Universidad Politécnica de Valencia, 46071-Valencia, Spain
e-mail: hgarcia@vega.cc.upv.es

[2] Chemistry Department, University of Ottawa, K1N 6N5, Canada

Abstract. Diffuse reflectance spectra of HY (Si/Al 15) and Hß (Si/Al 13) zeolites after adsorption of 1,1-diphenylethylene (DPE) show an intense 605-nm absorption band characteristic of an elusive blue species observed a long time ago for DPE-silica-alumina solids. This blue species was wrongly attributed to the corresponding $DPE^{+\bullet}$ radical cation or a complex of DPE with Lewis sites of these solids. In our case, EPR spectra of DPE samples adsorbed on HY and Hß zeolites indicate that the spin population of these samples is too low ($<10^{15}$ spin $\bullet$ g^{-1}) to contain significant amounts of any paramagnetic species. In addition, IR spectra of the organic material incorporated within HY and Hß is very similar to those of some DPE dimers. Product studies after solid-liquid extraction of zeolites and silica-alumina in which DPE has been adsorbed also show the formation of the corresponding dimers derived from the acid-catalyzed mechanism. Variable amounts of oxidation products are also formed when the adsorption is carried out in the open air. In addition, ^{13}C-NMR spectra in solution of blue samples generated by treatment of DPE with sulfuric acid in dimethyl sulfate also indicate the presence of the same dimer distribution and the absence of detectable low-field signals that could be attributed to any carbenium ion. With these data, it is clear that in spite of the intense color developed in these samples, the bulk of the organic material adsorbed on the zeolites does not correspond to any intermediate, but to dimers. Semiempirical ROHF calculations using the ZINDO program provide some support to the possibility that the blue color could be due to 1,1,3,3-tetraphenyl-1-butylium cation, the reaction intermediate involved in the DPE dimerization mechanism.

INTRODUCTION

In a seminal work, Rooney and Pink established in 1962 that adsorption of polynuclear aromatic hydrocarbons onto the surfaces of silica-alumina gives rise to the generation of the corresponding radical cations by single electron transfer from the organic substrate to the oxidizing sites of the solid.[1] Since this pioneering work, the ability of solid inorganic supports such as silica, alumina and aluminosilicates to spontaneously generate radical cations by mere adsorption of neutral precursors has been confirmed by a multitude of additional examples.[2, 3]

Zeolites possess a chemical composition identical to amorphous silica-alumina, but differ from them in the strict crystalline structure characteristic of zeolites with micropores of molecular size.[4] Much work has been done concerning the synthesis, modification and properties of zeolites since 1960. As consequence of this intensive research, many experimental techniques have been developed to fully characterize the structure, composition, nature of the sites and activity of zeolites.[5] Today, zeolites have become the solids of choice and have completely replaced silica and aluminas for most of their former catalytic applications.[6]

Formation of radical cations of arenes,[7-10] olefins,[11, 12] dienes,[13] conjugated α,ω-diphenyl polyenes,[14] amines,[8, 15] heterocycles[16, 17] and even saturated hydrocarbons[18] by adsorption within acid zeolites is now well documented. Therefore, the fact that radical cations can be generated by adsorption of electron-rich organic molecules is without question.

However, in the original article of Rooney and Pink besides polycyclic aromatic compounds, the case of 1,1-diphenylethylene (DPE) was also studied.[1] The resulting blue species after its adsorption on silica-alumina was characterized by EPR and also assigned to hydrated $DPE^{+\bullet}$ radical cation by analogy with other aromatic compounds. This blue species on silica-alumina possess in its UV/Vis absoption spectrum a strong absorption band at 600-nm having a shoulder on the short-wavelength side of the band.

In fact, the nature of the blue species arising from DPE has attracted much attention in the sixties trying to understand the acidic nature of silica-alumina surfaces.[19-32] Thus, it was later observed that the EPR signal of these blue samples is too weak to contain a significant spin population, ruling out the presence of significant amounts of a radical cation in these samples. On the other hand, the influence of DPE concentration on the intensity of the blue band seems to indicate a dimeric nature for this elusive species.[19, 20]

Other structures such as a π-complex between DPE and the Lewis sites of the solid[33-36] or a free carbenium ion have been alternatively proposed for this intriguing blue species (see Chart 1). In this context, Rooney and Hathaway suggested the allylic structure **1** to explain the absorption band at such long wavelengths in the visible.[37] But these structures have been never supported by complementary product studies, after desorption of the organics, that may shed some light on the nature of the processes involved. In addition, in more recent years $DPE^{+\bullet}$ and $(DPE)_2{}^{2+}$ have been conclusively generated and identified by means of pulse radiolysis.[38-40] Their corresponding UV/Vis spectra definitely do not correspond to the blue species responsible for the 600-nm band.

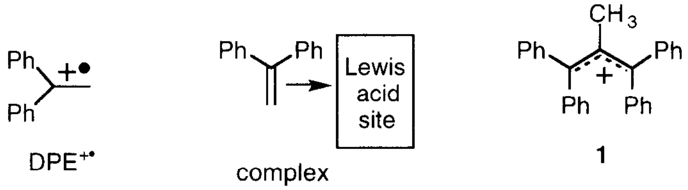

Chart 1

In the present work, we have adsorbed DPE onto a series of well-characterized zeolites of different topology and acid strength. The same blue species previously observed by Rooney and Pink was formed as a persistent intermediate within certain zeolites. As far as we know this is the first time that this species has been generated and stabilized on zeolites. We have acomplished a diffuse reflectance (DR), IR and EPR spectroscopic characterization of the organic material incorporated in the zeolite. Our characterization of the solids have been complemented with product studies as well as ^{13}C-NMR spectroscopy of solutions containing the blue species in dimethyl sulfate. The results show that the blue species only accounts for a minor portion of the material adsorbed on the solids, which contain a large amount of neutral dimeric compounds. A reasonable structure in agreement with the product distribution and theoretical calculations is proposed.

RESULTS AND DISCUSSION

Adsorption of DPE onto a series of zeolites was performed either by stirring isooctane solutions of DPE in the presence of thermally dehydrated zeolite or by heating progressively up to 150 ^{o}C a mechanical mixture of DPE and untreated zeolite. For DPE adsorptions onto the non-acidic Na$^+$-form of the Y zeolite, no color was observed immediatly after treatment, although by aging over days a light bluish tint was developed.

In contrast, for the H$^+$-form of zeolites in which their micropore system contains cages and cavities of large dimensions (zeolites Y and ß) (see Chart 2), the samples become blue in color. For these samples, the corresponding DR spectra completely agree with that previously reported by Leftin and Hall for the blue species derived from DPE[20] (Figure 1A). This blue species adsorbed on tri- or bidirectional zeolites was remarkably persistent, and we did not notice any apparent change in the spectra of these samples stored under aerobic conditions for days, although after longer periods an appreciable fading of the samples could be observed.

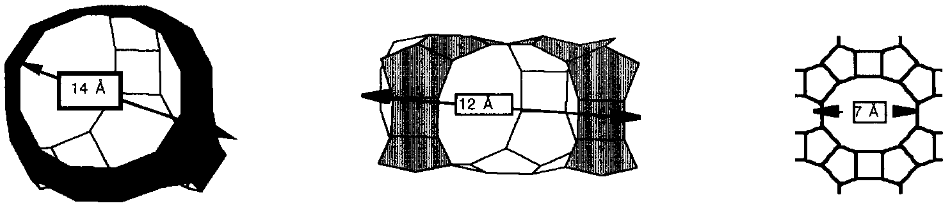

Faujasite Y supercavities

Zeolite Beta cages

Monodirectional channels of Mordenite

Chart 2

On the other hand, H$^+$-zeolites whose crystalline structure does not possess large internal voids did not exhibit the blue color. Particularly, when the adsorption was carried out after dehydration of monodirectional Mordenite or bidirectional medium-pore sized ZSM-5 zeolites, a band peaking at 450-nm was observed on top of a very broad structureless absorption covering the entire range of wavelengths (Figure 1B). The 450-nm species decays rapidly in the presence of moist air, indicating that it reacts readily with water. Taking into account the strong acidity of Mordenite and ZSM-5 as well as the chemical behavior of DPE, we assign the 450-nm to 1,1-diphenylethylium ion (DPEH$^+$) generated by protonation of the C=C double bond.[41, 42] Related diphenylmethylium cation has already been observed as transient species upon the photolysis of 1,1-diphenylacetones in dealuminated HY zeolite,[43] as well as pillared clays.[44]

To further characterize DPEH$^+$, we have performed a laser flash photolysis study in solution by irradiating DPE in trifluorethanol. The ability of this solvent to protonate C=C double bonds upon photolysis of styrenes is well-established,[45-47] and, thus, the band at 430-nm in the transient spectrum that is not quenched by oxygen can be confidently assigned to DPEH$^+$ (Figure 2).

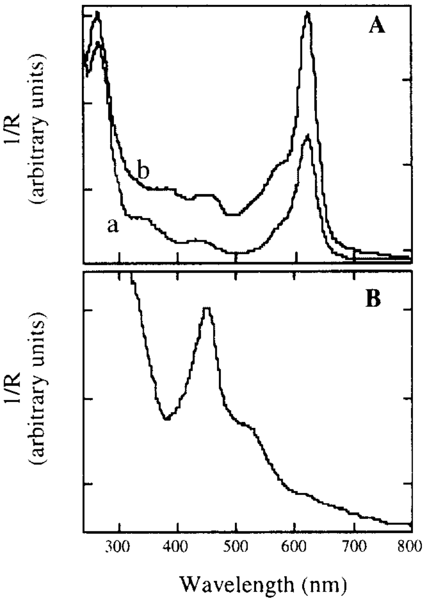

Figure 1. Diffuse reflectance spectra of DPE adsorbed on: A) large pore tridirectional HY (spectrum a) and Hß (spectrum b); B) monodirectional HMordenite zeolite. While the characteristic absorption band of the blue species at 605-nm accompanied with another absorption at 260-nm can be seen in spectra A, it is absent in the case of HMordenite (B), where an absorption at 450-nm attributable to DPEH$^+$ is observed.

A reasonable assumption to rationalize the different behavior of Mordenite and ZSM-5 compared to Y or ß protonic zeolites is based on the different dimensions of their micropores, not on the different nature of the intermediates involved in the process. Thus, DPEH$^+$ would be generated as the primary species in both type of zeolites, but while in Mordenite or ZSM-5 the more restricted reaction cavity would preclude its transformation to a bulkier secondary intermediate (probably by reaction with DPE, *vide infra*), the latter process could occur for voids of larger dimensions like those of Y or ß zeolites.

Concerning the possible radical cation nature of the blue (605-nm) species, our own quantitative EPR studies established that the signals of the blue intermediate adsorbed on dealuminated HY are very weak compared to samples containing other authentic radical cations that we have previously generated in Y zeolites.[16, 17] In agreement with the data reported for silica, our estimations indicates that the spin population must be lower than 10^{15} spin x g^{-1}. This means that if the blue species were an intermediate with an unpaired electron, their content would be around 10^{-4} mg per g of solid (assuming a formula weight of 360 daltons for a dimer) and the estimated apparent extinction coefficient for the 605-nm band should be in region of 10^6 M^{-1} cm^{-1}, which is very unusual for this type of absorptions in the visible.

Moreover, it was found that the absorption bands corresponding to DPE$^{+\bullet}$ and $(DPE)_2{}^{2+}$ appear at 550 and 520-nm, respectively.[39, 40] None of these maxima agree with that of the blue species (605-nm). Besides the dimer, no other species derived from DPE$^{+\bullet}$ has ever been reported. Therefore, it is unlikely that formation of the blue species involves an electron transfer mechanism.

In addition, we performed the selective poisoning of the oxidizing sites of Hß zeolite with thianthrene (E_{OX} = 1.23V vs SCE),[48] and observed that the characteristic blue color was still developed upon subsequent adsorption of DPE (E_{OX} = 1.46 V vs SCE)[49] onto thianthrene-doped Hß zeolite. This would indicate that the sites involved in the generation of the blue color are different of those others responsible for the single electron-acceptor ability of zeolites.

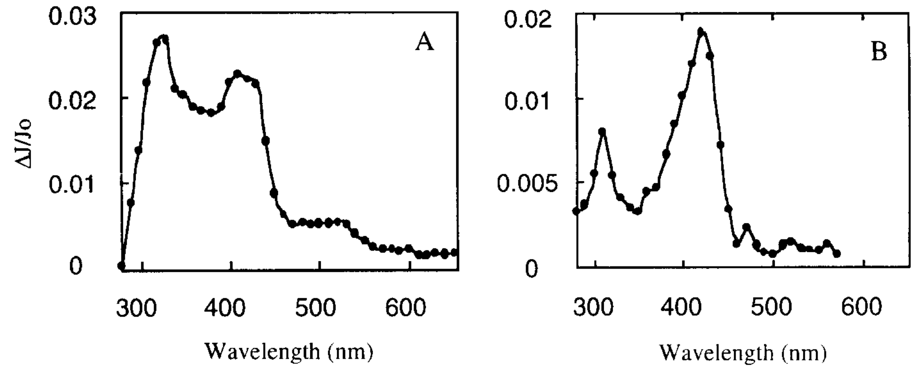

Figure 2. Transient spectrum of a solution of DPE in trifluoroethanol 1 μs after 266 nm excitation: A 30 min of N_2 purging; B purging with O_2. The bands at 325, 430 and 520-nm can be assigned to $DPEH^•$, $DPEH^+$ and $DPE^{+•}$, respectively.

In order to gain some insight in the nature of these intermediates, we performed product studies after adsorption of DPE onto the zeolites. In spite of the differences observed in the diffuse reflectance spectra for tri- and monodirectional zeolites (see Figure 1), the product distribution for most of the experiments followed a similar pattern. It consisted of variable mixtures of the open olefinic dimer **3** and the indanic cyclic dimer **4** (Scheme 1). Other minor oxidation products (particularly benzophenone) were also isolated and identified, but careful purging with N_2 or Ar of the zeolites remarkably decreases the yield of these adventitious products. Notably, adsorption of DPE onto silica-aluminas (25 or 75 wt % of Al_2O_3), which was the system originally studied by Rooney and Pink, gives rise the same product distribution of **3** and **4**.

The fact that the blue species can be generated even under the more strict anaerobic conditions (where benzophenone was formed only in trace amounts) indicates that this species is not related with any oxidation pathway.

Concerning compounds **3** and **4**, it is known that dimerization of styrene derivatives exhibit a variety of reaction mechanisms involving the intermediacy of carbenium ions, radicals or radical cations.[50, 51] It has been established that the actual dimer distribution is a fingerprint for each of these operating mechanisms. Therefore, by mere analysis of the dimer structures it is possible to ascertain the nature of the intermediate involved in the process. In our case, dimers **3** and **4** correspond to the products of an acid-catalyzed pathway.[33, 52] Interestingly, no cyclobutane or tetralin dimers **5**-**7** (Chart 3) could be detected, arguing against the intermediacy of $DPE^{+•}$.[53, 54]

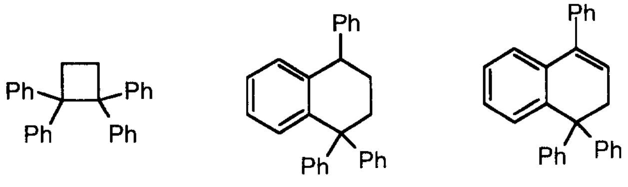

5 **6** **7**

Chart 3. Characteristic dimers of an electron transfer mechanism.

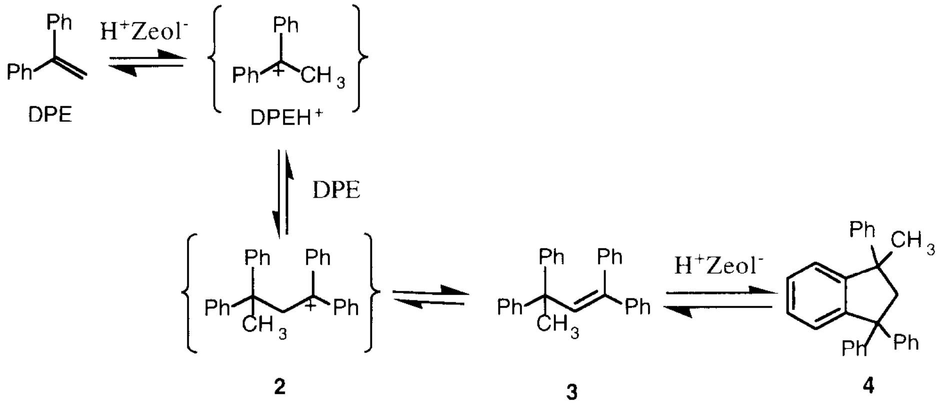

Scheme 1. Dimers observed after adsorption of DPE on acid zeolites.

IR spectroscopy is a powerful technique to investigate organic species adsorbed within zeolites. In the absence of water, the only absorption of the zeolite lattice corresponds to the Si-O stretching appearing around 1050 cm^{-1}. Therefore, zeolites are transparent in the zone characteristic of the main organic functional groups, allowing direct observation of the organic guests embedded within the aluminosilicate solid matrix. We have recorded IR spectra of samples containing the blue species (Figure 3), and observed that these spectra are compatible with the IR corresponding to dimers **3** and **4**, which are the products obtained after extraction of the blue zeolite samples. Thus, the aromatic region of the blue sample exhibit four main absorptions at 1593, 1560, 1500, and 1455 cm^{-1} also present although much sharper in the IR of pure dimers **3** and **4**. As it can be seen in Figure 3, the aromatic region (1700-1400 cm^{-1}) of compounds **3** and **4** is very similar making it difficult to establish the definite composition of the material present in the zeolite. Notably, no other species besides **3** and **4** has to be invoked to interpret the IR data of Figure 3A.

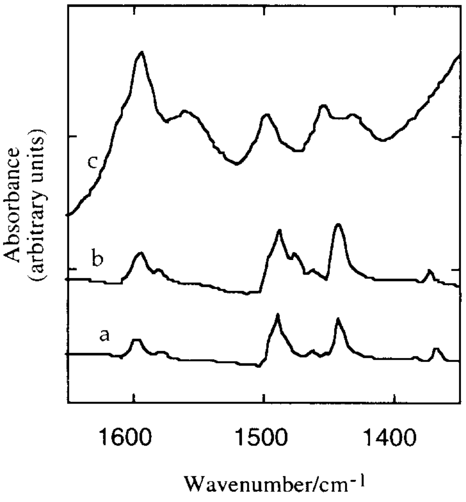

Figure 3. Aromatic region of the FT-IR Spectra of the linear dimer **3** (a) and the cyclic dimer **4** (b) in KBr disk. Spectrum c corresponds to the organic material present in the blue Hβ zeolite after incorporation of DPE. The last sample was outgassed at 100°C under 10^{-2} Pa for 1h prior to IR recording at room temperature.

In the same direction, no other compounds besides DPE and **3** were observed when the blue species was generated in the liquid phase. It has been reported that the UV/Vis spectrum corresponding to the blue species can be alternatively obtained by adding small amounts of sulfuric acid to a solution of DPE in dimethyl sulfate.[22] We have been able to reproduce this experiment and subsequently submit these samples to ^{13}C-NMR spectroscopy (Figure 4). All the signals of this mixture can be assigned either to unreacted DPE or to the dimer **3**. Attempts to obtain evidence for any carbenium ion that could be responsible for the color failed. After standing, a white solid recrystallized from these solutions, whose structure corresponds to dimer **4**. Benzophenone or any other oxidation product was also absent in the homogeneous phase experiments.

In addition, ^{13}C-NMR spectra of blue dimethyl sulfate solutions were also recorded at increasing concentrations of sulfuric acid and even in 96% sulfuric acid without dimethyl sulfate. Color changes of the solutions were observed, and eventually they became yellow. Under these more acidic conditions, spectra contaning the signals previously reported for DPEH$^+$ were recorded. The most characteristic singlet of DPEH$^+$ corresponds to the positive carbon at 229 ppm.[55]

Combination of the results obtained by IR spectroscopy of the zeolites as well as ^{13}C-NMR of the blue solutions clearly indicates that the species responsible for this color must be present only in very small amounts, and does not correspond to the bulk material of the adsorbed guest, which mainly contains dimers **3** and **4**.

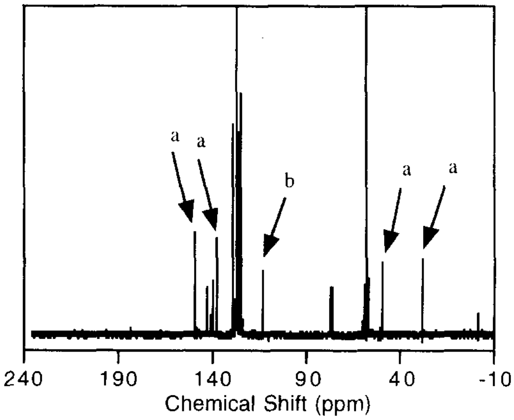

Figure 4. ^{13}C-NMR spectrum of blue solutions (UV/Vis spectrum showing an intense band at 605-nm) prepared by dissolving DPE (10 mg) in dimethyl sulfate (2 ml) containing H_2SO_4. The most characteristic carbons corresponding to the linear dimer **3** and DPE have been labelled with the letters a and b, respectively.

Taking into account the product distribution after adsorption on the zeolites, and the reaction mechanim outlined in Scheme 1, we especulate if the blue species could be any of the cationic intermediates involved in the dimerization. In particular, since DPEH$^+$ can be ruled out as the blue species based in its very different absorption spectrum, (Figure 2B) we addressed the possibility that the dimeric intermediate **2** or any carbenium ion derived from it could have a spectrum similar to that of Figure 1A.

In this regard, we have been unable to detect any product in wich a rearrangement of the methyl group respect to the structure of **2** has taken place. In particular, we were trying to establish the presence of compound **8** (Scheme 2). Neverthless, we performed calculations at the semiempirical level exploring the posibility that the allylic cation **1** suggested by Rooney and Hathaway could be responsible for the blue color.

The most resonable pathway to generate the allyl cation **1** from intermediate **2** is outlined in Scheme 2. According to this Scheme, while the following steps to generate **1** from **2** appears to be highly favorable, semiempirical AM1 calculation predicts that the initial hydride migration from **2** leading to 1,1,3,3-tetraphenylbut-2-ylium would be endergonic by 31.1 Kcal mol^{-1}. However, this value is not sufficiently high to conclusively rule out this possibility.

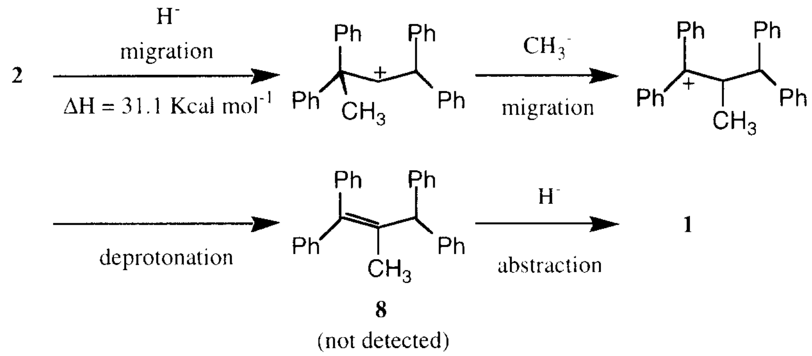

Scheme 2. Most reasonable pathway for allyl cation formation.

We focused also on intermediate **2** as responsible for the absorption spectrum shown in Figure 1A. According to the analogous chromophoric structure of DPEH$^+$ and **2**, one should expect a similar absorption spectrum for both cations, unless the two distal phenyl groups far from the positive center are somehow involved in the charge delocalization.

In order to address this possibility, we performed semiempirical AM1 ScF-MO calculations for structure **2**. In a subsequent step we applied the ZINDO program to the optimized AM1 geometry of **2**. ZINDO is free to modify the initial AM1 geometry and allows to predict the UV/Vis spectrum of an organic species. The resulting optimized ZINDO conformation as well as the partial charge corresponding to each atom is presented in Figure **5**. Notably, the formal positive charge of the trivalent carbon is predicted to be largely distributed through the distant moiety of the intermediate **2**. This contrasts with the results obtained by applying the same methodology to DPEH$^+$, in which a large partial positive charge is still retained on the trivalent carbon. Comparison of calculated structures of DPEH$^+$ and **2** indicates that the phenyl rings at the 3 position are playing a role in delocalizing the positive charge and therefore interacting with the trigonal carbon.

The UV/Vis spectrum for intermediates DPEH$^+$ and **2** was then calculated. Thus, while in good agreement with its experimental absorption spectrum, ZINDO does not predict for DPEH$^+$ any absorption above 500-nm, Figure **5** presents the results obtained for carbenium ion **2**. As can be seen there, the calculated spectrum of **2** possesses an unexpected broad band in the visible extending from 550 to 800-nm and peaking around 650-nm. Although it is reasonable to assume that the exact wavelength of the maximum would depend on the polarity and other solvatochromic effects experienced by **2** within the zeolite voids, what is remarkable is the difference in the calculated absorption spectra of DPEH$^+$ and **2**, in spite of having in common the benzhydryl substructure. We believe that the visible band arises from the participation of the distal phenyl rings in the charge delocalization of the positive trivalent carbon.

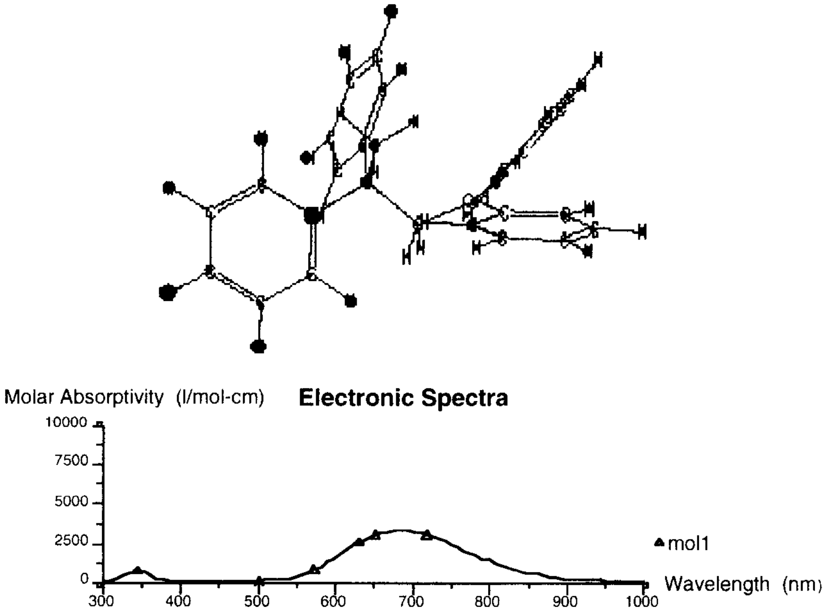

Figure 5. Optimized geometry of 1,1,3,3-tetraphenyl-1-butylium ion **2**. The size of the atomic radii has been plotted proportional to the local positive charge. The lower plot shows the ZINDO predicted UV/Vis spectrum for this cation where an absorption band in the visible is expected in contrast with the UV band (λ<500-nm) calculated for DPEH$^+$.

Likewise, we have calculated the UV/Vis absorption spectra of related structures analogous to **2**, all of them encompassing a ß-phenyl ring with respect to a positive benzylic moiety. Among the carbenium ions that we have studied, many others such as 3-methyl-1,1,3-triphenyl-1-butylium, 2,4,4-triphenyl-2-pentylium and 4-methyl-2,4-diphenylpentylium ions also exhibit in the predicted absorption spectrum a visible band at λ>500-nm showing that the phenomenon observed for **2** is more general and not restricted exclusively to this intermediate.

CONCLUSIONS

Upon adsorption of DPE on tridirectional large-pore zeolites, the solids developed the characteristic diffuse reflectance spectra previously observed for DPE on amorphous silica-alumina catalysts. EPR spectra established that no significant population of paramagnetic species are present in these blue zeolites. IR spectroscopy of these samples shows that the bulk organic material present in the zeolite matrix correspond to dimers, in agreement with the product distribution recovered after solid-liquid extraction. Therefore, the blue species must be present only in minute amounts as the ^{13}C-NMR spectra in solution indicates. According to semiempirical calculations, the reaction intermediate **2** involved in the acid-catalyzed dimerization of DPE can be a reasonable candidate to account for the characteristic color of these systems. However, the allylic intermediate **1** cannot positively disregarded.

EXPERIMENTAL

NaY was a commercial sample (Union Carbide SK-40, Si/Al 2.6). HY was obtained by steam dealumination at 300ºC of the previously NH_4^+ exchanged Y zeolite; the Si/Al ratio measured by chemical analysis was 15. Hß was prepared by thermal decomposition (500ºC, N_2 stream, 2 h) of an as-synthesized sample containing tetraethylammonium template according to reported procedures.[56] HMordenite was obtained by heating a suspension of commercial NaMordenite (PQ Industries, Si/Al 6) in 1 M hydrochloric acid for 30 min[52] and then washing thoroughly the solid with distilled water until no precipitation of Cl^- with an aqueous 0.1 M solution of $AgNO_3$ took place. ZSM-5 was synthesized following the patent literature[57] and calcined at 550 ºC under N_2 to decompose the tetrapropylammonium template, forming the protonic ZSM-5 zeolite.

Dehydration of zeolites was accomplished by heating at 500ºC overnight. Adsorption of DPE (40 mg) was carried out by stirring at room temperature an isooctane solution (30 ml) in the presence of dehydrated zeolites (1.00 g) for 30 min. Alternatively, a mechanical mixture of DPE (20 mg) and hydrated zeolite was progressively heated up to 150ºC and then the temperature maintained for 30 min.

Diffuse reflectance spectra were recorded in a Shimadzu UV-2101 PC scanning spectrophotometer using an integrating sphere. EPR measurements were carried out in a Bruker ER 200 D spectrometer at X-band (9.4-9.8 MHz) using DPPH ($g = 2.0036$) as standard. IR spectra of zeolites containing organic material were obtained using a Nicolet 710 FT-IR spectrophotometer in self-consistent wafers (10 mg) after outgassing at 200ºC and 10^{-2} Pa for 1 h. IR of pure compounds were recorded in KBr disks with the same instrument. Nanosecond laser flash set-up is similar to those previously described in detail.[58, 59] Photolyses of DPE in trifluorethanol (Aldrich) (O.D. = 0.2 at 266-nm) were carried in static quartz cells out using the 266-nm output of a Nd-YAG laser (5 ns, 10 mJ/pulse). The solutions were purged with N_2 or O_2 for 30 min prior to the photolysis.

For product studies, the solids were submitted to continuous solid-liquid extraction in a micro Soxhlet equipment using CH_2Cl_2 as solvent. The liquid phase was analyzed by GC (Hewlett-Packard 5890 provided with a 25 m capillary column of 5 % phenylmethylsilicone) and GC-MS (Hewlett-Packard 5988A same column and conditions as GC). Isolation of pure dimers **3** and **4** was accomplished with column chromatography using silica gel (Merck, 60 mesh) and a mixture as hexane-dichloromethane (5:1) as solvent. ^1H and ^{13}C-NMR were recorded in $CDCl_3$ using a 300 MHz Varian Geminis spectrometer with a SAM work station. Spectroscopic properties of **3** and **4** are coincident wint those previously reported.[60]

The optimization of the geometry of 1,1-diphenylethylium, 1,1,3,3-tetraphenyl-1-butylium and related cations was done by a semiempirical AM1 method using the MOPAC 94 program package, as a part of the CAChe system on the Macintosh IIvx computer. The eigenfunction following method was used in gradient minimization, to a gradient lower than 0.1. The optimized geometry was utilized to generate the electronic spectra using the configuration interaction routine implemented in the ZINDO program. The ROHF method was used with a INDO/2 parametrization of the Hamiltonian.

ACKNOWLEDGEMENTS

Financial support by the Spanish DGICYT (Grant no. PB93-0380) and partially by the European Comission within the Program of Human Capital and Mobility (CHRX-CT93-0280) is gratefully acknowledged. VM also thanks to the Generalidad Valenciana for a postgraduate scholarship. We are indebted with Prof. J. C. Scaiano for the facilities given to do part of this work and Dr. J.V. Folgado for EPR recording.

REFERENCES

1. Rooney, J.J.; Pink, R.C., *Trans. Faraday Soc.* **1962**,*58*, 1632-1641.
2. Bard, A.J.; Ledwith, A.; Shine, H.J. Formation, Properties and Reactions of Cation Radicals in Solution. *Adv. Phys. Org. Chem.* 1976 Academic Press. London.
3. Rhodes, C.J. Electron Spin Resonance. *Annual Reports on the Progress of Physical Chemistry.* 1993 Royal Society of Chemistry. London.
4. *Introduction to Zeolite Science and Practice*, van Bekkum, H.; Flanigen, E.M.; Jansen, J.C. ed., Elsevier: Amsterdam, 1991.
5. Delgass, W.N.; Haller, G.L.; Kellerman, R.; Lunsford, J.H. *Spectroscopy in Heterogeneous Catalysis; Academic Press: New York*; 1979.
6. Corma, A., *Chem. Rev.* **1995**,*95*, 559-614.
7. Rhodes, C.J., *J. Chem. Soc., Faraday Trans.* **1991**,*87*, 3179-3184.
8. Chen, F.R.; Fripiat, J.J., *J. Phys. Chem.* **1992**,*96*, 819-823.
9. Liu, X.S.; Thomas, J.K., *Langmuir* **1993**,*9*, 727-732.
10. Caldararu, H.; Caragheorgheopol, A.; Russu, R., *Coll. Surf.* **1993**,*72*, 37-41.
11. Rhodes, C.J., *Coll. Surf. A* **1993**,*72*, 111-118.
12. Crockett, R.; Roduner, E., *J. Chem. Soc., Perkin Trans. 2* **1993**,1503-1509.
13. Roduner, E.; Crockett, R.; Wu, L.M., *J. Chem. Soc., Faraday Trans.* **1993**,*89*, 2101-2105.
14. Ramamurthy, V.; Caspar, J.V.; Corbin, D.R., *J. Am. Chem. Soc.* **1991**,*113*, 594-600.
15. Chen, F.R.; Fripiat, J.J., *Ninth International Zeolite Conference.* **1992**, I, 603-610.
16. Corma, A.; Fornés, V.; García, H.; Martí, V.; Miranda, M.A., *Chem. Mater.* **1995**,*7*, 2136-2143.
17. Folgado, J.-V.; García, H.; Martí, V.; Esplá, M., *Micropor. Mater.* **submitted**,.
18. Chen, F.R.; Fripiat, J.J., *J. Phys. Chem.* **1993**,*97*, 5796-5797.
19. Leftin, H.P., *J. Phys. Chem.* **1960**,*64*, 1714-1717.
20. Leftin, H.P.; Hall, W.K., *J. Phys. Chem.* **1960**,*64*, 382-383.
21. Leftin, H.P.; Hobson, M.C.; Leigh, J.S., *J. Phys. Chem.* **1962**,*66*, 1214-1216.
22. Leftin, H.P.; Hall, W.K., *J. Phys. Chem.* **1962**,*66*, 1457-1463.
23. Leftin, H.P.; Hobson, M.C.J., *Adv. Catal.* **1963**,*14*, 115-201.
24. Hall, W.K., *J. Catal.* **1962**,*1*, 53-61.

25. Terenin, A., *Adv. Catal.* **1964**,*15*, 227-284.
26. Dollish, F.R.; Hall, W.K., *J. Phys. Chem.* **1965**,*69*, 4402-4405.
27. Hirschler, A.E., *J. Catal.* **1963**,*2*, 428-439.
28. Hirschler, A.E., *J. Catal.* **1966**,*5*, 196-197.
29. Hodgson, R.L.; Raley, J.H., *J. Catal.* **1965**,*4*, 6-11.
30. Flockhart, B.D.; Pink, R.C., *J. Catal.* **1965**,*4*, 90-99.
31. Flockhart, B.D.; Scott, J.A.N.; Pink, R.C., *Trans Faraday Soc.* **1966**,*62*, 730-730.
32. Little, L.H. *Infrared Spectra of Adsorbed Molecules*; Willmer Brothers Limited: New York, 1966.
33. Evans, A.G.; Jones, N.; Thomas, J.H., *J. Chem. Soc.* **1955**,1824-1831.
34. Evans, A.G.; Jones, N.; Jones, P.M.S.; Thomas, J.H., *J. Chem. Soc.* **1956**,2757-2770.
35. Evans, A.G.; Jones, P.M.S.; Thomas, J.H., *J. Chem. Soc.* **1957**,104-111.
36. Grace, J.A.; Symons, M.C.R., *J. Chem. Soc.* **1959**,958-962.
37. Rooney, J.J.; Hathaway, B.J., *J. Catal.* **1964**,*3*, 447-450.
38. Shida, T.; Hamill, W., *J. Chem. Phys.* **1966**,*44*, 4372-4377.
39. Schmidt, J.; Bös, J.; Mai, H.; Decker, U.; Halbig, M., *Radiat. Phys. Chem.* **1985**,*26*, 543-545.
40. Schmidt, J.; Decker, U.; Teply, J.; Bös, J.; Mai, H., *Radiat. Phys. Chem. Part C* **1990**,*36*, 715 - 719.
41. Olah, G.A., *J. Am. Chem. Soc.* **1966**,1488-1495.
42. McClelland, R.A.; Kanagasabaphy, V.M.; Steenken, S., *J. Am. Chem. Soc.* **1988**,*110*, 6913-6914.
43. Cozens, F.L.; García, H.; Scaiano, J.C., *J. Am. Chem. Soc.* **1993**,*115*, 11134-11140.
44. Cozens, F.L.; García, H.; Gessner, F.; Scaiano, J.C., *J. Phys. Chem.* **1994**,*98*, 8494-8497.
45. McClelland, R.A.; Chan, C.; Cozens, F.; Modro, A.; S., S., *Angew. Chem., Int. Ed. Engl.* **1991**,*30*, 1337-1339.
46. Cozens, F.; Li, J.; McClelland, R.A.; Steenken, S., *Angew. Chem., Int. Ed. Engl.* **1992**,*31*, 743-745.
47. Das, P.K., *Chem. Rev.* **1993**,*93*, 119-144.
48. Jones II, G.; Huang, B.; Griffin, S.F., *J. Org. Chem.* **1993**,*58*, 2035-2042.
49. Ciminale, F.; Lopez, L.; Mele, G., *Tetrahedron* **1994**,*50*, 12685-12696.
50. Benito, A.; Corma, A.; García, H.; Primo, J., *Appl. Catal.: A* **1994**,*116*, 127-135.
51. Abrahams, B.F.; Hoskins, B.F.; Michail, D.M.; Robson, R., *NATURE* **1994**,*369*, 727-729.
52. Fajula, F.; Ibarra, R.; Figueras, F.; Gueguen, C., *J. Catal.* **1984**,*89*, 60.
53. Mattes, S.L.; Farid, S., *J. Am. Chem. Soc.* **1986**,*108*, 7356-7361.
54. Mattay, J.; Vondenhof, M.; Denig, R., *Chem. Ber.* **1989**,*122*, 951-958.
55. Olah, G.A.; Grant, J.L.; Spear, R.J.; Martin Bollinger, J.; Serianz, A.; Sipos, G., *J. Am. Chem. Soc.* **1975**,*98*, 2501-2507.
56. Camblor, M.A.; Mifsud, A.; Pérez-Pariente, J., *Zeolites* **1991**,*11*, 792-797.
57. Argauer, R.J.; Landlolt, G.R., *U.S. Pat.* **1982**,3 702 886.
58. Scaiano, J.C.; Tanner, M.; Weir, D., *J. Am. Chem. Soc.* **1985**,*107*, 4396-4403.
59. Banks, J.; García, H.; Miranda, M.A.; Pérez-Prieto, J.; Scaiano, J.C., *J. Am. Chem. Soc.* **1995**,*117*, 5049-5054.
60. Ciminale, F.; Lopez, L., *Tetrahedron Lett.* **1985**,*26*, 789-792.

(*Received in UK* 23 *December* 1996; *revised* 3 *February* 1997; *accepted* 6 *February* 1997)